CHARACTERIZATION OF DELAMINATION FRACTURE SURFACES UNDER MIXED MODE LOADING

R.M.M. Marat-Mendes [1], M.M. de Freitas [2]

[1] Escola Superior de Tecnologia de Setúbal, Campus do IPS,
Estefanilha, 2910-761 Setúbal, Portugal
e-mail: rmendes@est.ips.pt

[2] Instituto Superior Técnico, Universidade Técnica de Lisboa
Av. Rovisco Pais, 1049-001 Lisboa, Portugal
e-mail: mfreitas@dem.ist.utl.pt

ABSTRACT

Delamination is an important mode of failure on laminated composite materials and the characterization of this failure mode is a subject of research. Mode I, mode II, mode III and mixed-mode I+II fracture toughness were obtained using the double cantilever beam test (mode I), the end notch flexure test (mode II), the original and the modified edge crack torsion test (mode III) and the mixed-mode bending test (mixed-mode I+II) respectively. Fracture surfaces obtained during mode III interlaminar fracture toughness of glass/epoxy composites have been also studied using the original and the modified edge crack torsion test geometry. Results were compared with delaminating surfaces obtained during tests of mode I, mode II and mixed-mode I+II. In the original ECT test the hackle marks appears only in the side of the loading pin. In the modified ECT test the hackle marks appears in both sides of the sample and slightly less well defined and smoother fracture features in the middle of the sample.

KEY WORDS: Glass fibre epoxy, interlaminar fracture, fractographic analysis.

1. INTRODUCTION

Interlaminar damage (delamination) is one of the predominant forms of failure in many laminated composites systems. It is usually considered to be a crack propagation between two adjacent layers, in modes I, II or III, in the general case.

Analysis and test techniques for mode I delamination of a composite material have been extensively studied and the preferred technique to obtain the mode I partition is the Double Cantilever Beam test (DCB) [1]. Also mixed-mode I+II analysis and test techniques of laminated composite materials have been extensively studied and standardized with the Mixed Mode Bending test (MMB) [2,3]. Mode II partition has been also extensively studied but up to date, no standard method has been established for measuring mode II critical strain energy release rate, G_{IIC}. The End Notch Flexure (ENF) and the Four Point Bend End-Notch Flexure (4ENF) tests have shown to be the preferred test techniques to obtained mode II partition of the critical strain energy release rate [4-8]. Pure mode III test technique has not been yet achieved however a lot of work concerning mode III partition have been extensively presented in the literature [9-19]. The most recent test technique is the modified Edge Crack Torsion test (ECT) [20] which is a modification of the original Edge Crack Torsion test proposed initially by Lee [21].

In this study, the fracture surfaces obtained during mode III interlaminar fracture of glass/epoxy laminated composites have been investigated using the original and the modified ECT test geometry. It has been reported that with these specimens and test methods a mixed-mode II+III state exists at the delamination front, therefore special attention is focused on this characterization. The fracture surfaces obtained under ECT tests are compared with those obtained with DCB, ENF and MMB tests. The present study aimed at evaluating the adequacy of ECT specimen for the determination of mode III fracture toughness of a glass/epoxy material by combining experimental tests, numerical analyses and specimen fracture observations.

2. MATERIALS

The material used in this work is a unidirectional epoxy prepeg (ET443) reinforced with E glass fibre (UE400REM) supplied by Texipreg®. A 12.7 μm thick Teflon® foil was inserted at the mid-plane of the panels during the lay-up process to define a starter delamination crack. The panels were cured at 125 ºC and 7 bar for 1 h.

The lay-up used in the DCB, ENF and the MMB tests is the one proposed by the mode I [1] and mixed-mode I+II standards [2] which is the $[0]_{24}$. The lay-up used in the ECT test is the $[90/(\pm 45)_3/(\mp 45)_3/90]_s$, this selection of ECT specimen lay-up and dimensions was made considering Li [22] and Carlsson [10] works. Li [22] reported consistent toughness values without transverse cracking problems on this specimen. This stacking sequence is more effective on avoiding transverse cracks in interface 90º plies than the one used recently by Ratcliffe [20], $[90/0/(\pm 45)_3/(\mp 45)_3/0/90]_s$,

Table 1. Lamina Properties.

Test	Lay-up	E_{11} [GPa]	$E_{22}=E_{33}$ [GPa]	$G_{12}=G_{13}=G_{23}$ [GPa]	$\nu_{12}=\nu_{13}$	ν_{21}	V_f [%]
DCB ENF MMB	$[0]_{24}$	43.94	16.71	6.57	0.300	0.114	58.16
ECT	$[90/(\pm 45)_3/(\mp 45)_3/90]_s$	43.42	9.49	6.57	0.316	0.069	56.55

since the incorporation of 0º plies reduces torsional stiffness and strength. Therefore, in view of the ply thickness of the present glass/epoxy material, the stacking sequence used was the one used by Li [22] and Carlsson [10]. Lamina properties were previously determined and are present in Table 1.

Specimens were cut from the panels and the DCB, ENF and MMB nominal dimensions were W=162 mm, b=25 mm with an initial delamination length of a=30 mm and a thickness of $2h$=6.5±0.7 mm (Figure 1). On the other hand, the selected ECT dimensions were L=89 mm, b=38 mm, with five groups of crack lengths $\tilde{a}$= 0, 8, 13, 19 and 23 mm and a thickness of $2h$=8.3±0.3 mm (Figure 2).

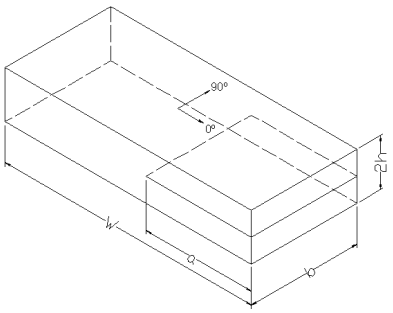

Figure 1. Schematic of DCB, ENF and MMB specimens.

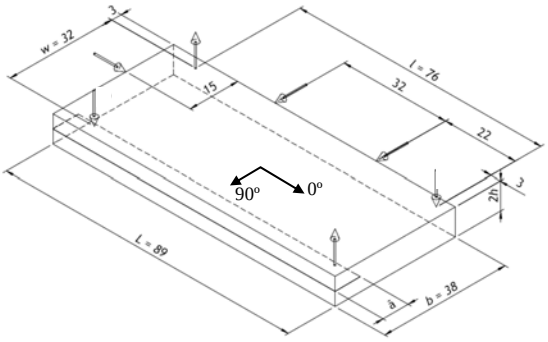

Figure 2. Schematic of ECT specimen.

3. EXPERIMENTAL PROCEDURE

The specimens have been mounted into the test fixtures and static tests were conducted under displacement control at a crosshead displacement rate of 0.5mm/min. This slow rate allowed crack propagation to be followed and recorded easily. Load-displacement plots were recorded during the tests. All fracture tests were performed from the end of the (straight) insert without pre-cracking the specimen.

Mode I, mode II, mixed-mode I+II and mode III fracture toughness were obtained using the DCB, the ENF, the MMB and the original and the modified ECT (O-ECT, M-ECT) tests respectively. The original ECT (O-ECT) fixture (Figure 3) provides supports at three points in three corners, guided by three guide pines to provide perfect alignment and the transverse load is introduced at the fourth point, the unsupported corner, by compression of the loading pin.

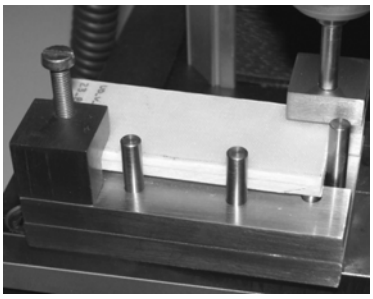

Figure 3. Original ECT test fixture

The modified ECT (M-ECT) test fixture is shown in Figure 4. The ECT specimen is supported in two supports in two corners, guided by three guide pines to provide perfect alignment and the transverse load is introduced symmetrically at the two unsupported corners, by compression of the loading pin.

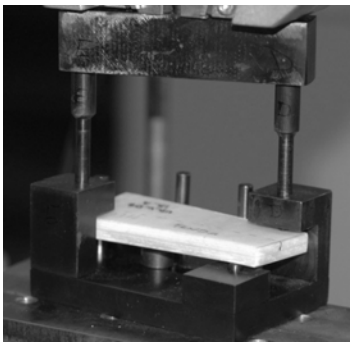

Figure 4. Modified ECT test fixture.

4. ANALYSIS

The virtual crack closure technique (VCCT) [23] was used to calculate the mode I, mode II and mode III strain energy release rate components. Table 2 shows

the fracture toughness obtained through the VCCT from the DCB, the ENF and the M-ECT tests.

Table 2 - Fracture toughness.

	G_{IC} [kJ/m^2]	G_{IIC} [kJ/m^2]	G_{IIIC} [kJ/m^2]
NL	0.845	1.272	0.946
5%/max	0.869	1.309	1.770

5. RESULTS AND DISCUSSION

A scanning electron microscopic (SEM) was used throughout this work to study the fractography of the broken specimens after DCB, ENF, MMB and ECT tests. The specimens were opened after testing and gold sputtering. Analysis of the fracture surfaces using SEM is necessary in order to obtain the maximum information possible concerning the fracture of ECT specimens and compare these fracture surfaces with the DCB, ENF and MMB specimens.

5.1. Mode I fractography

A typical scanning electron micrograph of the fracture surface in Mode I failure mechanism is characterized by fractures localised mainly in the resin and along the resin/fibre interface. SEM images of the crack surfaces in the starter region, Figure 5, clearly shows broken fibres pulled out from the resin as an evidence of the fibre bridging.

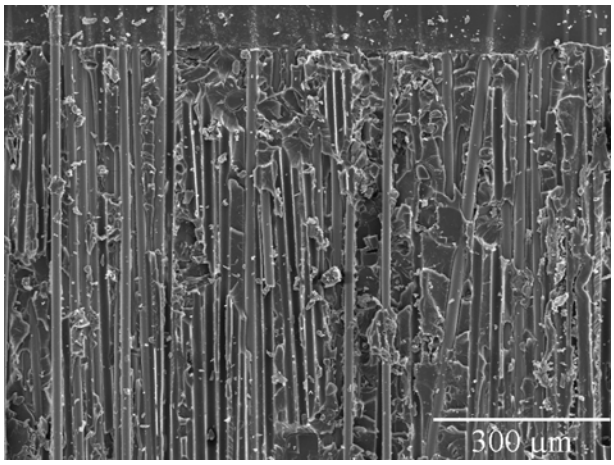

Figure 5. Scanning electron micrographs of DCB fracture surfaces. (Crack propagates from top to bottom).

5.2. Mode II fractography

Fracture surfaces shown in Figure 6 were formed by the characteristic hackle pattern, usually observed after mode-II failure. Mode II failure mechanism consisted of fibre breakage under shearing and is characterized by fractures localised in the resin with many hackles having an orientation of approximately 90º to fibre orientation.

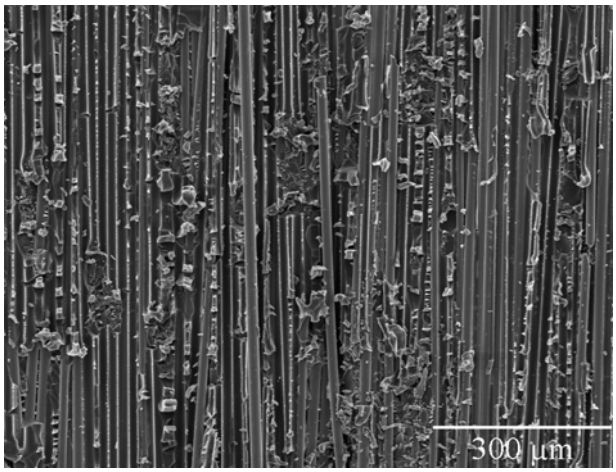

Figure 6. Scanning electron micrographs of ENF fracture surfaces. (Crack propagates from top to bottom).

5.3. Mixed-Mode I+II fractography

In the case of mixed-mode, the mechanisms is more complex consisted of fibre breakage under shearing (mode II) characterized by fractures localised in the resin with *hackles* having an orientation of 90º and others at less than 45º and also fractures localised in the resin and along the resin/fibre interface (mode I), Figure 7.

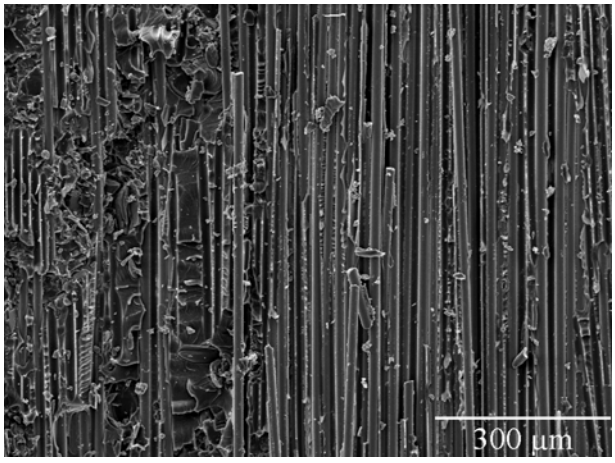

Figure 7. Scanning electron micrographs of MMB fracture surfaces (Crack propagates from top to bottom).

5.4. Mode III fractography

Fracture surfaces of the original and modified ECT specimens have been studied in three different positions. Fracture surfaces of the original ECT specimens have been analysed in the a) loading side, b) middle of the specimen and c) support side. The modified ECT fracture surfaces have been also analysed

in the a) loading side localized upper the starter film, b) middle of the specimen and c) loading side localized outside the starter film.
A schematic of the SEM locations of the fracture surfaces of the original ECT specimens is shown in Figure 8 for the a) loading side (*position 7*), b) middle of the specimen (*position 13*) and c) support side (*position 4*).

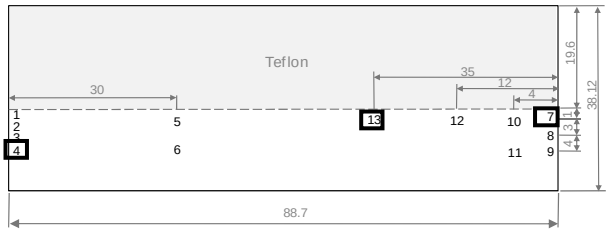

Figure 8. Schematic of the SEM locations of the original ECT sample.

Figure 9 shows the scanning electron micrographs in the side of the loading pin (*position 7* in Figure 8) where it is shown that the fracture surfaces of the original ECT specimens are very different from the fracture surfaces shown earlier in the DCB, ENF and MMB specimens. Here it is clear that the *hackles* are mainly orientated in approximately 45º to the fibre orientation, which indicates a mode III fracture. It can be also observed a presence of *hackles* with a 90º orientation, even in lower amount, like the ones observed in the ENF samples, which indicates a presence of a partition of mode II fracture.

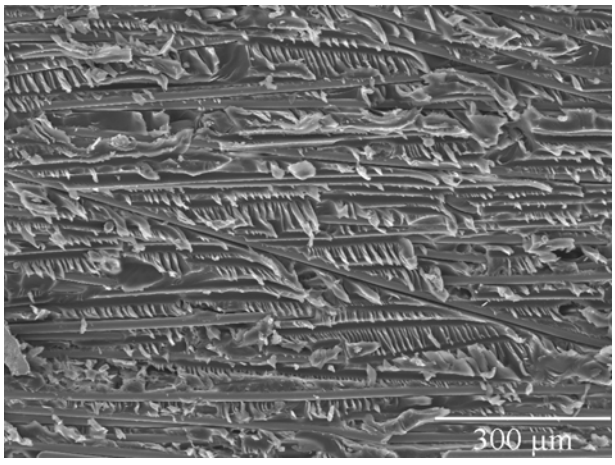

Figure 9. SEM of original ECT sample in the loading side (position 7) (Crack propagates from left to right).

Figure 10 shows the scanning electron micrographs in the middle of the specimen (*position 13* in Figure 8) where it is shown that the fracture surface of the original ECT specimen in this position is very different from the one shown in Figure 9. Here it can be seen that the *hackles* diminishes which indicates a diminishing of mode III presence.

Figure 11 shows the scanning electron micrographs in the support side (*position 4* in Figure 8) where it can be observed a presence of *hackles* orientated in approximately 45º to the fibre orientation indicating a mode III fracture, but this can be only observed when magnified.

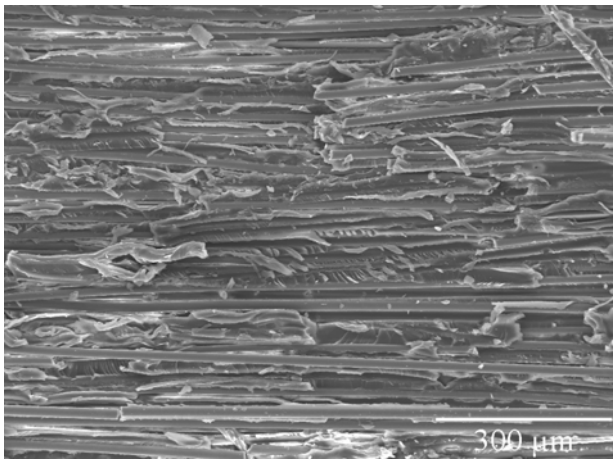

Figure 10. SEM of original ECT sample in the middle of the specimen (position 13) (Crack propagates from left to right).

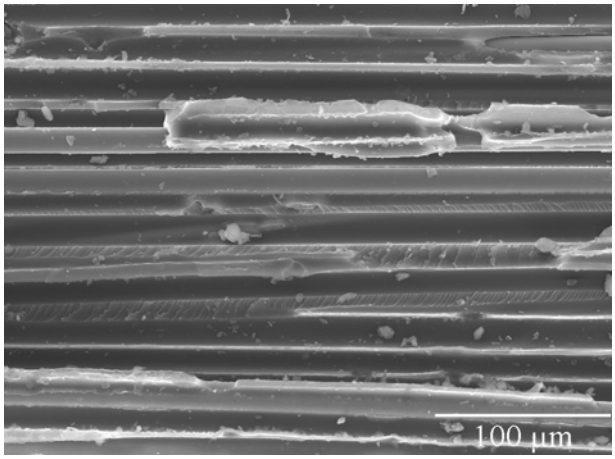

Figure 11. SEM of original ECT sample in the support side of the specimen (position 4) (Crack propagates from left to right).

A schematic of the SEM locations of the fracture surfaces of the modified ECT specimens is show in Figure 12 for the a) loading side localized upper the starter film (*position 1*), b) middle of the specimen (*position 17*) and c) loading side localized outside the starter film (*position 14*).

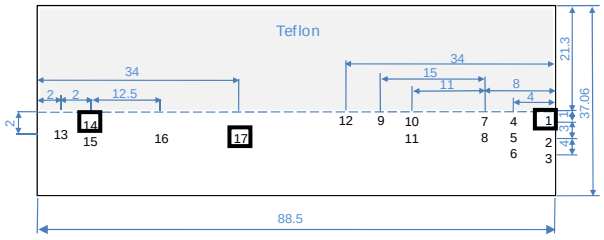

Figure 12. Schematic of the SEM locations of the modified ECT sample.

Figure 13 shows the scanning electron micrographs in the loading side localized upper the starter film (*position 1* in Figure 12) where it is shown that the fracture surfaces of the modified ECT specimens in this position is similar to the fracture surfaces observed in the same side of the original ECT specimen. These fracture surfaces are characterized by *hackles* orientated in approximately 45º to the fibre orientation, which indicates a mode III fracture and also a presence of *hackles* with a 90º orientation, even in lower amount, which indicates a presence of a partition of mode II fracture.

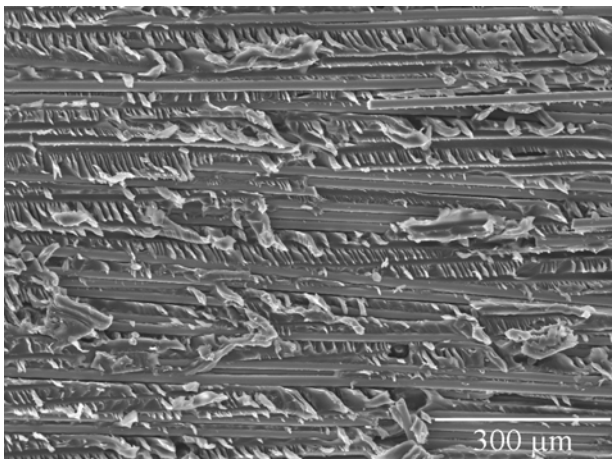

Figure 13. SEM of modified ECT sample in the loading side localized upper the starter film (position 1) (Crack propagates from left to right).

Figure 14 shows the scanning electron micrographs in the middle of the specimen (*position 17* in Figure 12) where it is shown that the fracture surface of the modified ECT specimen in this position is very different from the one shown in Figure 13. Here it can be seen that the *hackles* are less defined with smoother fracture features which indicates a diminishing of mode III presence.

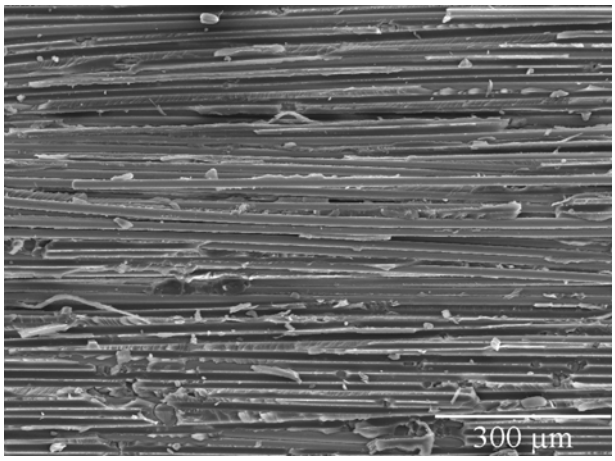

Figure 14. SEM of modified ECT sample in the middle of the specimen (position 17) (Crack propagates from left to right).

Figure 15 shows the scanning electron micrographs in the loading side localized outside the starter film (*position 14* in Figure 8) where it can be observed that the presence of the *hackles* orientated in 45º to the fibre orientation indicating a mode III fracture are similar to the ones observed in the side of the loading upper the starter film. These observations indicate that the modified ECT specimens present a mode III fracture in both sides of the specimen away from the middle of the specimen.

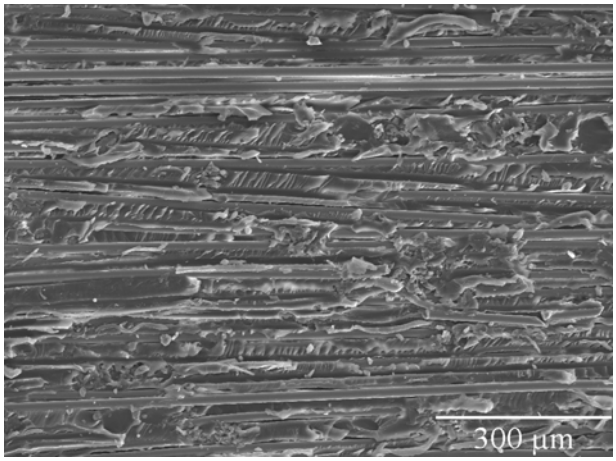

Figure 15. SEM of modified ECT sample in the loading side localized outside the starter film (position 14) (Crack propagates from left to right).

6. CONCLUSIONS

The present investigation has examined the fractographic features associated with delamination in glass/fibre laminated composite comparing the fracture surfaces of the original and modified ECT specimens with the DCB, ENF and MMB fracture surfaces.

The predominant fractographic feature found in mode I testing was broken fibres and pull-out from fibre bridging were observed. In mode II testing, the most predominant morphology was the hackle pattern perpendicular to the fibre orientation. In mixed-mode I+II testing, fractographic observation shows fibre breakage under shearing (mode II) characterized by fractures localised in the resin with *hackles* having an orientation of 90º and others at less than 45º and also fractures localised in the resin and along the resin/fibre interface (mode I).

The mode III fractographic observation shows predominant morphology with hackle pattern oriented at approximately 45º to the crack propagation direction. In the original ECT test the hackle marks appears only in the side of the loading pin. In the Modified ECT test the hackle marks appears in both sides of loading and less defined with smoother fracture features in the middle of the specimen. Mode III characterization concluded that some limited mixed-mode II+III seems to be present for ECT specimen on delamination initiation and growth, but a large majority of mode III delamination is present.

ACKNOWLEDGEMENTS

The authors thank the support from the Portuguese Foundation for Science and Technology (FCT) for the PhD grant no.SFRH/BD/25561/2005.

REFERENCES

[1] *ASTM D 5528 – 01 Standard Test Method for Mode I Interlaminar Fracture Toughness of Unidirectional Fiber-Reinforced Polymer Matrix Composites.* s.l. : American Society for Testing and Materials, 1994. Annual Book of ASTM Standards.

[2] *ASTM D 6671 – 01, Standard Test Method for Mixed Mode I-Mode II Interlaminar Fracture Toughness of Unidirectional Fiber Reinforced Polymer Matrix Composites.* s.l. : ASTM International, 2000.

[3] Marat-Mendes, R. and Freitas, M., *Mode I, mode II, mode III and mixed mode interlaminar fracture of glass/epoxy unidirectional laminates.* Porto, Portugal : Proceedings of EUROMECH 473, 2005.

[4] Blackman, B.R., Brunner, A.J. and Williams, J.G., *Mode II fracture testing of composites: a new look at an old problem.* Vol. 73, pp. 2443-2455, 2006.

[5] Davies, P., Casari, P. and Carlsson, L.A., *Influence of fibre volume fraction on mode II interlaminar fracture toughness of glass/epoxy using the 4ENF specimen.* Composites Science and Technology, Vol. 65, pp. 295-300, 2005.

[6] Pereira, A.B., et al., *Mode II interlaminar fracture of carbon/epoxy multidirectional laminates.* Composite Science and Technology, Vol. 64, pp. 1653-1659, 2004.

[7] Wang, J. and Qiao, P., *Novel beam analysis of end notched flexure specimen for mode-II fracture.* Engineering Fracture Mechanics, Vol. 71, pp. 219-231. 2004

[8] de Morais, A. B., *Analysis of mode II interlaminar fracture of multidirectional laminates.* Composites: Part A, Vol. 35, pp. 51-57, 2004.

[9] Farshad, M. and Flueler, P., *Investigation of mode III fracture thoughness using an anti-clastic plate bending method.* Engineering Fracture Mechanics, Vol. 60 (5-6), pp. 597-603, 1998.

[10] Li, X., Carlsson, L. A. and Davies, P., *Influence of fiber volume fraction on mode III interlaminar fracture toughness of glass/epoxy composites.* Composites Science and Technology, Vol. 64, pp. 1279-1286, 2004.

[11] Moura, M. F., et al., *Finite Element Analysis of the ECT Test on Mode III Interlaminar Fracture of Carbon Epoxy Composite Laminates.* 10th Portuguese Conference on Fracture, 2006.

[12] Moura, M.F., Silva, M.A. and Morais, J.J., *Análise Numérica do Ensaio ECT (Edge Crack Tortion) em Materiais Compósitos.* Granada, España : SEMNI, Congreso de Métodos Numéricos en Ingeniería, 2005.

[13] Pennas, D., Cantwell, W.J. and Compston, P., *The Influence of Strain Rate on the Mode III Interlaminar Fracture of Composite Materials.* Journal of Composite Materials, Vol. 41, pp. 2595-2614, 2007.

[14] Silva, M.A.; Moura, M. F.; Morais, A. B.; Morais, J.J., *Validação Numérica do Provete Edge Crack Torsion (ECT), para determinação experimental de G_{IIIC} em Materiais Compósitos de Carbono-Epóxido.* Ciência & Tecnologia dos Materiais, Vol. 18 (8), 2006.

[15] Suemasu, H. *An experimental method to measure the mode III interlaminar fracture toughness of composite laminates.* Composites Science and Technology, Vol. 59, pp. 1015-1021, 1999.

[16] Zhao, D. and Wang, Y., *Mode III fracture behavior of laminated composite with edge crack in torsion.* Theoretical and Applied Fracture Mechanics, Vol. 29, pp. 109-123, 1998.

[17] de Morais, A.B., Pereira, A.B., Moura, M.F., Magalhães, A.G., *Mode III interlaminar fracture of carbon/epoxy laminates using the edge crack torsion (ECT) test.* Composites Science and Technology, Vol. 69, pp. 670-676, 2009.

[18] Marat-Mendes, R. and Freitas, M., *Characterisation of the edge crack torsion (ECT) test for the measurement of the mode III interlaminar fracture toughness.* Engineering Fracture Mechanics, Vol. 76, pp. 2799–2809, 2009.

[19] Marat-Mendes, R. and Freitas, M., *Failure criteria for mixed mode delamination in glass fibre epoxy composites.* Composite Structures. doi:10.1016/j.compstruct.2009.07.017, 2009.

[20] Ratcliffe, J.G., *Characterization of the Edge Crack Torsion (ECT) Test for Mode III Fracture Toughness Measurement of Laminated Composites.* Langley Research Center, Hampton, Virginia: National Research Council, 2004.

[21] Lee, S.M., *An Edge Crack Tortion Method for Mode III Delamination Fracture Testing.* Journal of Composite Technology & Research, Vol. 15 (3), pp. 193-210, 1993.

[22] Li, J., Lee, S.M, Lee, E.W., O'Brian, T.K., *Evaluation of the Crack Tortion (ECT) Test for Mode III Interlaminar Fracture Toughness of Laminated Composites.* Journal of Composites Technology & Research, Vol. 19 (3), pp. 174-183, 1997.

[23] Ronal Krueger, *The Virtual Crack Closure Technique: History, Approach and Applications*, NASA/CR-2002-211628, April 2002.